

# Dynamic Interreceptor Coupling Contributes to the Consistent Open Duration of Ryanodine Receptors

Xin Liang,<sup>†</sup> Xiao-Fang Hu,<sup>†\*</sup> and Jun Hu<sup>†‡</sup>

<sup>†</sup>School of Life Science and Biotechnology, Shanghai Jiao Tong University, Shanghai, China; and <sup>‡</sup>Shanghai Institute of Applied Physics, Chinese Academy of Sciences, Shanghai, China

**ABSTRACT**  $\text{Ca}^{2+}$  spark is the elementary  $\text{Ca}^{2+}$  signaling event in muscle excitation-contraction coupling. The rise time of  $\text{Ca}^{2+}$  spark is rather stable under different conditions, suggesting consistent open duration of ryanodine receptors (RyRs) in vivo. It has been proposed that the array-based behavior of RyRs plays an important role in shaping  $\text{Ca}^{2+}$  spark dynamics, particularly in controlling the open duration of RyR clusters. Therefore, we investigated the possible role of inter-RyR coupling in stabilization of the open time of arrayed RyRs under several potential perturbations, for instance, array size, inter-RyR coupling noise, and up-regulation or down-regulation of the activity of partial RyRs in the array. We found that RyR arrays with dynamic coupling showed consistent open duration against the perturbations, whereas the RyR array with constant coupling did not. On the other hand, the open probability and amplitude of RyR arrays with dynamic interreceptor coupling were sensitive to the perturbations. These two points were consistent with experimental observations, indicating that the RyR array with dynamic coupling could recapitulate in vivo open properties of RyRs. Our findings support the idea that dynamic coupling is a feasible in vivo working mechanism of RyR arrays.

## INTRODUCTION

The ryanodine receptor/calcium release channel (RyR) is the ion channel mediating  $\text{Ca}^{2+}$  release from endoplasmic/sarcoplasmic reticulum (SR) and plays a pivotal role in intracellular  $\text{Ca}^{2+}$  signaling processes, such as excitation-contraction coupling, in all muscle cell types (1–4). RyRs usually form two-dimensional regular arrays in SR membranes (5–7). The quantitative measurement of  $\text{Ca}^{2+}$  sparks generated by coordinated activation of locally arrayed RyRs provides valuable information regarding in vivo gating of RyR arrays (8,9).

Among the properties of  $\text{Ca}^{2+}$  sparks, rise time (RT) is rather consistent under different conditions. First, the RT of  $\text{Ca}^{2+}$  sparks shows a weak correlation with the amplitude of sparks (10,11), indicating the lack of dependence of RT on the number of open RyRs. Second, the RT also shows weak or no sensitivity to multiple channel activity modulators. For instance, ATP is an activator of the RyR channel. The increase of ATP from 0.5 to 5.0 mM shows little effect on the RT of  $\text{Ca}^{2+}$  sparks, but induces ~33% enhancement of spark frequency and ~20% reduction of spark amplitude (12).  $\text{Mg}^{2+}$  is an inhibitor of RyR activity. The increase of  $\text{Mg}^{2+}$  to ~4 mM dramatically decreases the frequency of  $\text{Ca}^{2+}$  sparks, but still does not change the RT of  $\text{Ca}^{2+}$  sparks (13). A similarly consistent RT is also observed in the presence of other modulators (13–15). Since the RT of  $\text{Ca}^{2+}$  sparks closely reflects the open duration of RyRs, the stable RT against the perturbations suggests the robustness of the open duration of arrayed RyRs in vivo.

Although consistent RT of  $\text{Ca}^{2+}$  sparks is widely observed, the underlying mechanism is still unknown. In contrast to the stereotypical open time of RyRs in vivo (8), the open time of isolated and reconstituted single RyRs in vitro always follows exponential distributions (4,16,17), suggesting that the interreceptor functional coupling is involved in the opening of RyRs (9,18). Several inter-RyR coupling models have been proposed. Coupled gating, which proposes the simultaneous opening and closing of neighboring RyRs, assumes the constant coupling of neighboring RyRs (16,19). However, it has been found that constant coupling leads to prolonged opening of RyRs (16). In our previous work, we proposed a dynamic inter-RyR coupling model based on experimental observations and mathematical simulations (20,21). In this model, inter-RyR coupling is dynamically modulated according to channel functional states (21). The inter-RyR coupling is strong at rest to stabilize the RyR arrays in the closed state, and the coupling strength is decreased when it accompanies the activation of RyRs to facilitate the rapid termination of  $\text{Ca}^{2+}$  release.

In this work, we further investigated whether dynamic inter-RyR coupling contributed to the consistent open duration of RyR arrays. We compared the open properties of arrayed RyRs with either constant coupling or dynamic coupling in the presence of several perturbations, including differing array size, inter-RyR coupling noise, and up-regulation or down-regulation of the activity of partial RyRs in the array. We found that the RyR array with dynamic coupling exhibited consistent open duration against these perturbations, whereas the RyR array with constant coupling did not. These results support the concept that dynamic coupling is a feasible in vivo working mechanism of RyR arrays.

Submitted December 21, 2008, and accepted for publication March 26, 2009.

\*Correspondence: xfh@sjtu.edu.cn

Editor: Richard W. Aldrich.

© 2009 by the Biophysical Society  
0006-3495/09/06/4826/8 \$2.00

doi: 10.1016/j.bpj.2009.03.042

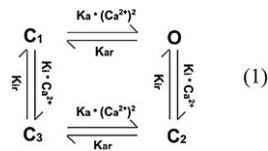
## MODELING AND METHODS

### Basic model

The model basically adopted the dynamic coupling (DC) model that we established previously (21). Here, we describe it briefly as a synthesis of the single-channel gating model, the 2-D RyR array model with key parameters  $e$  and  $\alpha$ , and the SR calcium release model.

#### The single-channel gating model

The effects of both activation and inactivation of  $\text{Ca}^{2+}$  on the activity of RyRs were considered. Given the law of conservation of mass and energy, we built a four-state scheme to describe RyR gating (Eq. 1), including three closed states ( $C_1$ ,  $C_2$ , and  $C_3$ ) and one open state (O).



The detailed information and kinetics parameters of this simplified model were the same as listed in Fig. 1 B and Table 1 of our previous work (21).

#### The 2-D RyR array model

Typically, the square lattice formed of 25 ( $5 \times 5$ ) receptors was adopted, except when discussing the size of the RyR array. Intermolecular coupling was introduced into the kinetics of arrayed RyRs through a coupling coefficient (Eq. 2):

$$K_{ij} = k_{ij} \times \exp^{\sum_{m=1}^n (e_{jsm} - e_{ism}) / (kT)}, \quad (2)$$

where  $K_{ij}$  is the kinetic parameter of coupled RyRs;  $k_{ij}$  is the kinetic parameter of isolated RyRs;  $e_{ij}$  is the interaction energy between two contacting RyRs;  $ij$  is the current/next state of the central RyR;  $s_m$  is the state of a neighboring RyR; and  $n$  represents the number of physical contacting neighbors of the central RyR.

Furthermore, a coefficient matrix was constructed to modify the interaction energy ( $e$ ) between neighboring RyRs in a state-dependent manner (Eq. 3):

$$e_{ij}/kT = \begin{pmatrix} & \text{C}_1 & \text{O} & \text{C}_2 & \text{C}_3 \\ \text{C}_1 & 1 & -1 & -1 & -1 \\ \text{O} & -1 & \alpha & -\alpha & -1 \\ \text{C}_2 & -1 & -\alpha & \alpha & -1 \\ \text{C}_3 & -1 & -1 & -1 & 1 \end{pmatrix} \times e. \quad (3)$$

Detailed information about this matrix has been described previously (21). As the most important parameter,  $\alpha$  is the coefficient for the interaction energy between two RyRs bound to activating  $\text{Ca}^{2+}$  (states O or  $\text{C}_2$ ) and could be adjusted to simulate the state-dependent coupling behavior.

#### The SR calcium release model

The in situ SR calcium release model adopted the model used in our previous work (21). Several different spatial regions were considered. The  $\text{Ca}^{2+}$  dynamics in all the spaces were formulated in the earlier study (21) and the value of all the parameters could be found in Table 2 of that article (21).

#### $e$ and $\alpha$

According to our previous work, the key parameters in the DC model were set according to Eq. 4. In addition to the DC model, the constant coupling (CC) model was used here as a control mechanism (Eq. 4). In our previous work,  $e$  was 0.45 for the optimal signal/noise ratio in both the DC and CC

models.  $\alpha$  was 0.6 in the DC model and 1.0 in the CC model to simulate different inter-RyR couplings when channels were opened.

$$\begin{array}{ll}
 \text{DC:} & (e, \alpha) = (0.45, 0.6) \\
 \text{CC:} & (e, \alpha) = (0.45, 1.0).
 \end{array} \quad (4)$$

### Parameters and calculation

Several other parameters were recorded to evaluate the performance of RyR arrays in signaling, described as follows:

1. Open duration, the duration of a single opening event.
2. Amplitude  $\text{RyR}_{\text{open}s}$ , maximum number of  $\text{RyR}_{\text{open}}$  channels during one opening event of an array.
3. Resting  $P_o$ , average open probability of arrayed RyRs in the resting state. This parameter was averaged from at least 50 simulations (the recording time of one simulation is usually  $\sim 10^7$  time steps (biological time, 1 s), much longer than the duration of an array opening event).

All these parameters were presented as the average  $\pm$  SD of at least 50 simulations.

### Variables

The potential physiological perturbation was simulated by modifying the parameters accordingly. The details were described as follows.

#### Size of RyR array

Previous studies have shown that the size of the RyR array varied in the range 10  $\sim$  100, depending on the muscle type and the species (5). Therefore, arrays formed of 9 ( $3 \times 3$ )  $\sim$  100 ( $10 \times 10$ ) RyRs were all included. For simplification, all arrays were square (Fig. 1 A). Several other size-related parameters were also modified accordingly.

1. The volume of the subspace ( $V_{\text{SS}}$ ) was related to array size based on Eq. 3 in our previous work (21).
2. The number of L-type  $\text{Ca}^{2+}$  channels was related to array size according to the RyR/dihydropyridine receptors ratio in cardiac muscle cells ( $\sim 7.3$ ) (22).
3. No experimental data are available on how the volume of junctional SR ( $V_{\text{JSR}}$ ) changed for arrays of different sizes. Therefore, we simply used the size-independent  $V_{\text{JSR}}$  when changing the array size. We also did simulations with the size-dependent  $V_{\text{JSR}}$ . It was found that although the JSR volume affected the termination speed of the RyR array, it did not affect our conclusions on the effects of dynamic coupling on consistent open duration of the array.

#### Noise of inter-RyR coupling

The thermal noise of inter-RyR coupling was introduced into the simulation by modifying the key parameter  $e$  (interaction energy) as follows:

$$\begin{array}{l}
 e' = e' \times n(1, \delta) \\
 \text{if}(n(1, \delta) < 0) \rightarrow n(1, \delta) = 0.
 \end{array} \quad (5)$$

In Eq. 5,  $n(1, \delta)$  is a noise coefficient that obeys the normal distribution with a mean value of 1 and an SD of  $\delta$ . If the stochastically generated noise coefficient was negative, we set it to be 0. After being modified by the noise coefficient,  $e$  was not a constant number but a group of normally distributed numbers (Fig. 2 A). Since the value of  $\delta$  could affect the amplitude of stochastic fluctuation, we used  $\delta$  to evaluate the noise intensity in the presentation of results, below.

#### Functional modulation of individual RyRs

In this part of the simulation, we let the program randomly select some RyRs in the array before the experimental simulations and then applied special

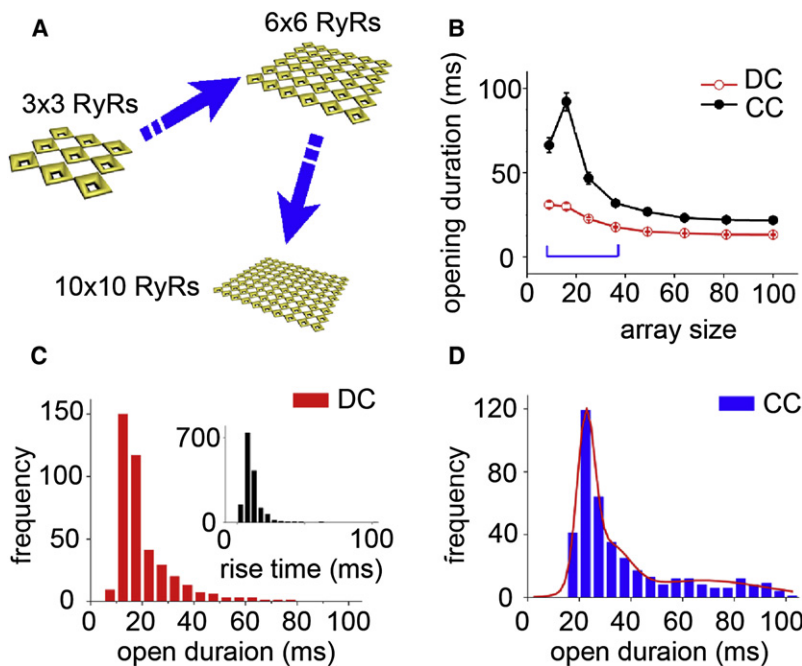


**FIGURE 1** Open duration of RyR arrays with different sizes. (A) Cartoon schemes of arrays with different sizes (from  $3 \times 3$  to  $10 \times 10$  RyRs). (B) The size-dependent curves of array open duration with the CC and DC models. (C) Statistical distribution of the open duration of RyR arrays with sizes of  $3 \times 3$ ,  $4 \times 4$ ,  $5 \times 5$ , and  $6 \times 6$  RyRs when the DC model was adopted. Data from 50 simulations were collected for arrays of each size. (Inset) Histogram of  $\text{Ca}^{2+}$  spark RT of rat ventricular myocytes ( $\text{Ca}^{2+}$  spark data were provided by Prof. Zhu Peihong, Shanghai Institute for Biological Sciences, [phzhu@sibs.ac.cn](mailto:phzhu@sibs.ac.cn)). (D) Statistical distribution of the open duration of RyR arrays with sizes of  $3 \times 3$ ,  $4 \times 4$ ,  $5 \times 5$ , and  $6 \times 6$  RyRs when the CC model was adopted. Data from 50 simulations were collected for arrays of each size.

rules to these selected RyRs. The inactivation and activation of some RyRs were simulated in this part, and the details were as follows.

Inactivation (Fig. 3 A) was applied to simulate the situation in which some RyRs were constantly bound with certain inhibitors, e.g.,  $\text{Mg}^{2+}$ . Since  $\text{Mg}^{2+}$  could bind to the inhibition site of RyRs, the selected RyRs would remain in the  $\text{C}_3$  state (see Fig. 1 B in our previous article (21)) and could never be activated by  $\text{Ca}^{2+}$ .

Up-regulation of activity (Fig. 3 C) was applied to simulate the situation where some RyRs were constantly activated by certain factors, e.g., ATP and  $\text{Ca}^{2+}$ . The activation constant ( $k_{\text{on}}$ ) of selected RyRs (i.e., the “on” rate of activating  $\text{Ca}^{2+}$ ; see Table 1 in our previous work (21)) was increased (~1.5-fold) to enhance the activity of RyRs.

## Computation

The operation of the RyR lattice array during SR calcium release was run based on cellular automata and the Monte Carlo method with a time step of  $10^{-7}$  s. All programs were allowed to run for a period of time (usually  $2 \times 10^6$  time steps, or a biological time of 200 ms) for stabilization before the beginning of experimental simulations. All codes for this model were written in Fortran and operated on a Dell workstation for scientific computation.

## $\text{Ca}^{2+}$ spark imaging and data analysis

All the  $\text{Ca}^{2+}$  spark data (in rat cardiac myocytes) were obtained from the laboratory of Professor Peihong Zhu (Shanghai Institute for Biological Sciences, Shanghai, China). The methods have been described previously (23). In brief, the isolated rat ventricular myocytes were loaded with fluo-4 AM for 30 min at  $25^\circ\text{C}$ . Then, the cells were perfused with an experimental solution of (in mM) NaCl 135, KCl 5.4,  $\text{MgCl}_2$  2.1,  $\text{NaH}_2\text{PO}_4$  0.33, HEPES 5, glucose 10, and  $\text{CaCl}_2$  1.0, pH 7.4 (NaOH) at  $25^\circ\text{C}$  for 30 min to deesterify fluo-4 AM before recording.  $\text{Ca}^{2+}$  sparks were observed by laser scanning confocal microscopy (MRC 1024, Bio-Rad, Hercules, CA) equipped with a  $60\times$  oil immersion objective (numerical aperture 1.4). During recording, the intact myocytes were continuously perfused with experimental solution. Fluo-4 was excited at a wavelength of 488 nm, and fluorescence was measured at  $>522$  nm. The parameter setting for  $\text{Ca}^{2+}$  imaging (e.g., laser intensity, gain) was kept constant in all experiments. For analyzing the kinetics of  $\text{Ca}^{2+}$  sparks, the XT line scanning mode was adopted. The scanning line had 512 pixels, with an actual length of  $51.2 \mu\text{m}$ , and was oriented along the long axis of the myocyte, with the nucleus avoided. A full image was obtained by stacking scanning lines, which required ~1 s (~2 ms/line). The images were automatically processed as previously described (23). Briefly,  $\text{Ca}^{2+}$  sparks were identified as local

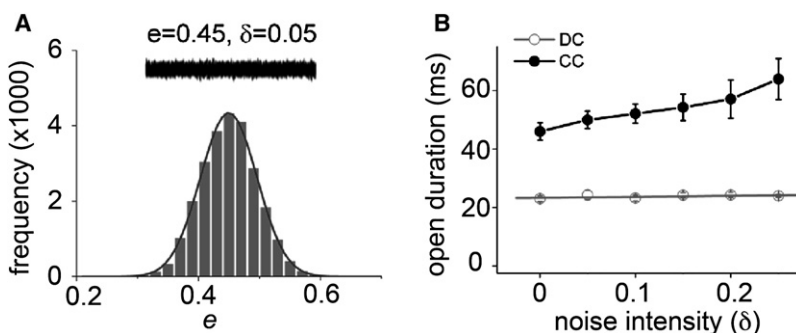


**FIGURE 2** Effect of inter-RyR coupling noise on open duration of the RyR arrays. (A) The normally distributed inter-RyR coupling noise. (B) The noise-intensity-dependent curves of open duration of RyR arrays with the DC and CC models. A  $5 \times 5$  RyR array was used in the simulations.

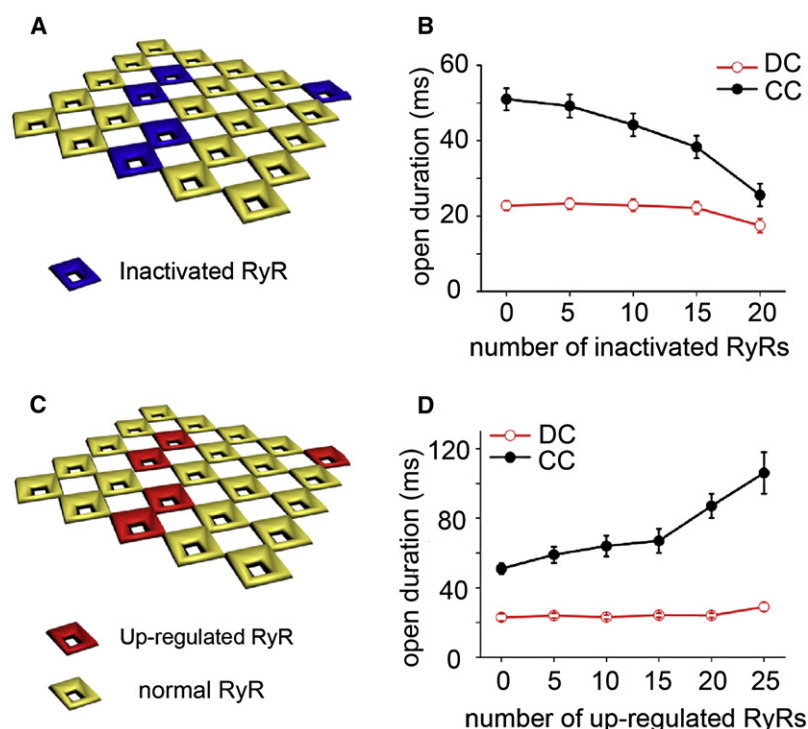


FIGURE 3 Effect of inactivation or activation of partial RyRs on the open duration of the RyR array. (A) Cartoon scheme of the RyR array with some inactivated RyRs. (B) Dependence of the open duration of a  $5 \times 5$  RyR array on the number of inactivated RyRs in the array with the DC and CC models. (C) Cartoon scheme of an RyR array in which the activity of some RyRs is up-regulated. (D) Dependence of the open duration of a  $5 \times 5$  RyR array on the number of up-regulated RyRs in the array with the DC and CC models.

peak elevations of fluorescence intensity ( $F$ ), which were  $>3\times$  the SD of the surrounding resting fluorescence ( $F_0$ ). The measured time to peak intensity (RT) of  $\text{Ca}^{2+}$  sparks was used as an estimation of RyR array opening duration in vivo.

## RESULTS

### Consistent open duration

We compared the open time of RyR arrays, using either constant coupling or dynamic coupling in the presence of different perturbations.

#### Different array size

Electron microscope studies indicate that the number of RyRs in the lattice usually varies between 10 and 100, depending on the species and muscle type (5,7). The observation that no correlation exists between the amplitude and temporal parameters of  $\text{Ca}^{2+}$  sparks (10,11) suggests that the open duration of the array is independent of the array size. Therefore, we first tried to test which inter-RyRs coupling model could produce the weak size-dependent behavior of array open duration.

The open durations of RyR arrays of different sizes (from 9 RyRs ( $3 \times 3$ ) to 100 RyRs ( $10 \times 10$ )) were collected and compared. When the CC model was adopted, the open duration of the RyR array was significantly related to array size (Fig. 1 B). The open duration increased when array size was increased from 9 to 16 RyRs. The open duration then dramatically decreased when the array size became larger. When the DC model was adopted, the open duration showed

less dependence on the array size (Fig. 1 B) and only a slight decrease with the increase of array size. This slight reduction of open duration was due to the faster depletion of SR  $\text{Ca}^{2+}$  with the increased number of arrayed RyRs.

Considering that  $\text{Ca}^{2+}$  sparks are usually generated by a cluster of 5–40 RyRs (24–26), we focused on array sizes from  $3 \times 3$  to  $6 \times 6$  RyRs. We collected the open durations of arrays within this range to make the statistical distribution. The histogram of open time of RyR arrays with the DC model showed a single-peak profile (Fig. 1 C), whereas that with the CC model showed a multi-peak distribution, with an open duration  $>100$  ms (Fig. 1 D). Compared to the RT distribution of  $\text{Ca}^{2+}$  sparks, which was collected from rat ventricular myocytes (Fig. 1 C, inset), it was obvious that the results from the DC model were more similar to experimental observations.

#### Thermal noise of inter-RyR coupling

Previous electronic microscopy studies have shown the structural overlap between two physically coupled RyRs (5,6,18). In principle, the structural interaction on the nanometer scale would be easily affected by the thermal noise, for instance, through fluctuation of the structure at the molecular level. Therefore, the thermal noise of inter-RyR coupling would be a perturbation that might disturb the gating properties of the RyR array. In principle, this effect should be influenced by the change of temperature. However, a study of how temperature affects  $\text{Ca}^{2+}$  sparks showed that the RT of  $\text{Ca}^{2+}$  sparks is quite stable in the temperature range of 20–35°C (27). Thus, it is interesting to examine which model



could cause the array to have consistent open duration under the influence of thermal perturbation.

Since it was difficult to precisely simulate the complex thermal noise that existed in the neighboring RyRs, for simplification, we summarily considered the total noise by introducing a normalized noise coefficient (Fig. 2 A, and see [Modeling and Methods](#) for details). After the modification, the value of  $e$  (interaction energy) (Fig. 2 A) would fluctuate around the mean value (optimal value,  $e = 0.45$ ) (21) and the amplitude of fluctuation could be modulated by adjusting the intensity of the noise coefficient ( $\delta$ ). It was found that in the DC model, the noise of inter-RyR coupling did not have obvious effects on the open duration of the RyR array ( $5 \times 5$ ). Even when the noise intensity ( $\alpha$ ) increased to  $\sim 0.25$ , the open duration of the array remained  $\sim 23$  ms (Fig. 2 B). However, if the inter-RyR coupling was always kept strong, e.g., in the CC model, the noise of inter-RyR coupling would obviously affect the open duration of the array. With the increase of noise intensity from 0 to 0.25, the open duration increased from  $\sim 49$  ms to  $\sim 65$  ms in a nearly linear manner.

#### *Altered activity of partial RyR channels*

In vivo observations of  $\text{Ca}^{2+}$  sparks show that the open duration of RyRs is rather consistent against channel activity regulators, such as  $\text{Mg}^{2+}$ , ATP, etc. (12–15). In this section, we examine the open duration of the RyR array ( $5 \times 5$ ) with both the CC and DC models in the presence of some inactivated or activated RyRs.

First, we tested the effects of inactivated RyRs on the open duration of the RyR array. In muscle cells, there was  $\sim 1$  mM  $\text{Mg}^{2+}$  in the cytoplasm (13).  $\text{Mg}^{2+}$  competed with  $\text{Ca}^{2+}$  to bind to RyRs and inactivate the channels even in the resting state (4,13). Previous studies have shown that up to 4 mM  $\text{Mg}^{2+}$  could alter only the frequency, but not the rise time, of spontaneous  $\text{Ca}^{2+}$  (13). According to the affinity of  $\text{Mg}^{2+}$  for RyRs ( $\sim 1$  mM) (4), some RyRs should be inactivated in the presence of 4 mM  $\text{Mg}^{2+}$ . In our work, we changed the number of inactivated RyRs in the  $5 \times 5$  array to mimic the increased inactivation effect (Fig. 3 A). As shown in Fig. 3 B, when constant coupling was applied, the open duration was decreased with an increase in the number of inactivated RyRs in the array. When the number of inactivated RyRs increased to 20 (at which time only 5 RyRs in the 25 RyR array remained excitable), the open duration of the RyR array dramatically decreased from  $\sim 49$  ms to  $\sim 25$  ms. In contrast, with dynamic coupling, the RyR array showed consistent open duration in the presence of the inactivation effect. Even when the number of inactivated RyRs increased to 20, the mean open duration only decreased from  $\sim 23$  ms to  $\sim 21$  ms in the DC model.

Next, we tested the effects of RyR channel activation on the open duration of the RyR array with the DC and CC models. The open duration of the RyR array was also insensitive to activators, like micromolar cytoplasmic  $\text{Ca}^{2+}$ , ATP,

calmodulin, etc. (12,13,15). Therefore, we further tested the performance of the array when the activity of some RyRs was up-regulated (Fig. 3 C). We enhanced the activity of some RyRs by increasing the  $k_{\text{on}}$  of activating  $\text{Ca}^{2+}$  by 1.5-fold. It was found that in the CC model, the open duration rapidly increased with the increase of up-regulated RyRs in the array. When all the RyRs were up-regulated, the open duration was prolonged to  $>100$  ms. When the DC model was applied, the open duration remained stable at  $\sim 23$  ms (Fig. 3 D). Even when the activity of all RyRs was up-regulated, the open duration was only prolonged to  $\sim 28$  ms, showing higher robustness in the presence of agonists. However, it should be stated that such robustness was affected by the extent of up-regulation and the number of up-regulated RyRs. For instance, if the extent of up-regulation was to be further increased by a factor of 2.0, the open duration would only remain consistent when the number of up-regulated RyRs was  $<10$  and would increase to  $\sim 40$  ms when all RyRs were up-regulated in the DC model ( $>150$  ms in the CC model under this condition). Therefore, compared to the CC model, the open duration of the RyR array in the DC model is still highly robust.

In the above simulations, some RyRs in the array were stochastically selected to be inactivated or up-regulated. In fact, the spatial position in the array of the RyRs selected also had some effects on the final properties of the RyR array. However, for the RyRs selected with specific spatial positions, our conclusion as to the robustness of the open duration would not be affected.

#### **Tunable open probability and amplitude**

The above simulation results showed that with the DC model, the RyR array exhibited consistent open duration against multiple potential perturbations. To have a complete view on the performance of the array in the presence of perturbations, we further investigated the open probability and response amplitude of the RyR array with dynamic inter-RyR coupling, and correlated these parameters to the frequency and amplitude, respectively, of  $\text{Ca}^{2+}$  sparks. By measuring all these parameters, we may obtain a deeper understanding of how the system adjusts its activity to respond to regulators or disturbances.

First, we found that with dynamic coupling, open probability and open amplitude of the RyR array showed higher sensitivity to array size. When array size increased from 9 to 100 RyRs, the spontaneous open probability of the array decreased from  $\sim 5 \times 10^{-3}$  to  $\sim 2 \times 10^{-3}$  (Fig. 4 A, circles), showing that large arrays were more stable in the resting state. Meanwhile, the output amplitude of large RyR arrays was higher than that of small arrays (Fig. 4 A, triangles), which was obviously due to the increased number of open channels. These results clearly indicate that compared to open duration, open probability and open amplitude were more sensitive to the change in array size.

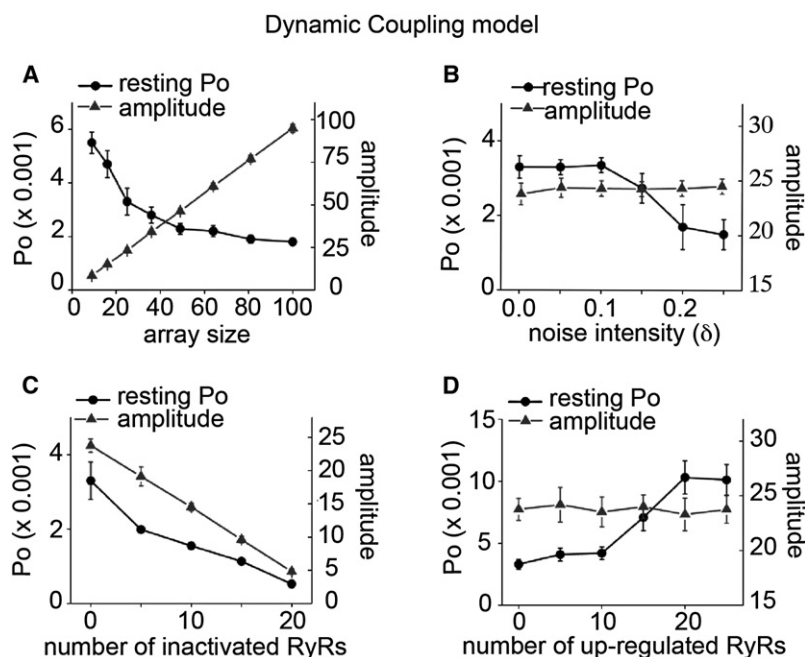


FIGURE 4 Open probability and open amplitude of the RyR array with dynamic coupling in the presence of different perturbations, including changes in array size (A) and inter-RyR coupling noise (B), inactivation of some RyRs in the array (C), and up-regulation of the activity of some RyRs in the array (D).

Second, we investigated the response of the RyR array ( $5 \times 5$ ) to the noise of inter-RyR coupling. We found that, similar to open duration, the output amplitude of the array was insensitive to the potential thermal noise of inter-RyR coupling (Fig. 4 B, triangles). However, it was noted that the spontaneous open probability of the array showed a decreasing behavior with an increase in coupling noise (Fig. 4 B, circles). When the intensity of the noise was weaker than 0.1, the spontaneous open probability of the array remained nearly stable. But when the noise intensity was  $>0.1$ , the resting open probability noticeably decreased. When the noise intensity reached 0.25, the resting open probability of the array decreased to  $1 \times 10^{-3}$  (Fig. 4 B). Noise is usually defined as demolishing the stability of the system. It was interesting that here the coupling noise could enhance the stability of the RyR array, which should be favored by the array system during its evolution.

Third, we tested the effect of inactivation/activation of partial RyRs on the open probability and open amplitude of the RyR array ( $5 \times 5$ ). It was found that along with the increased number of inactivated RyRs, both the resting  $P_o$  and the output amplitude decreased. When 20 RyRs in the array were inactivated in the  $5 \times 5$  RyR array, the resting open probability was reduced from  $3 \times 10^{-3}$  to  $5 \times 10^{-4}$  (Fig. 4 C, circles). Meanwhile, the open amplitude also decreased (Fig. 4 C, triangles) with the increase of inactivated RyRs. These phenomena resulted from the decrease of excitable RyRs in the array.

In the fourth scenario, the output amplitude of the RyR array was relatively consistent against the number of RyRs with up-regulated activity (Fig. 4 D, triangles), since the arrays always fully opened. However, the resting open probability of the array showed a biphasic tendency. The curve

first showed a plateau phase with  $<10$  up-regulated RyRs and then exhibited a stage of increase when the number of RyRs with up-regulated activity increased (Fig. 4 D, circles). The results suggest that due to the stability of the RyR array in the resting state, the agonists would not immediately cause enhancement of RyR activity. Only when the up-regulation exceeds the threshold does the activity of the arrayed RyRs further increase. The joint point of these two phases, in principle, largely relies on the strength of the activation effect.

Compared to open duration, the open probability and open amplitude of the RyR array with dynamic coupling are more tunable to the perturbations. These results are consistent with the tunable parameters of frequency and amplitude of  $\text{Ca}^{2+}$  sparks under different conditions (10–15).

## DISCUSSION

In this study, we have shown that the DC model endows the array system with relatively consistent open duration in the presence of potential perturbations, including variations of array size, inter-RyR coupling noise, and up-regulation or inactivation of partial arrayed RyRs. Therefore, it is necessary to discuss why the DC model could help the array to achieve a consistent open duration against multiple modulators.

In fact, the physiological modulators of the 2-D RyR array can be divided into two classes. The first class exerts its effect at the level of the entire array, e.g., the array size and the coupling noise. Changing the array size alters the average inter-RyR coupling strength and, thus, the total coupling strength of the RyR array. The different-sized arrays are differently affected by the geometry of the array.

Larger arrays are less affected by boundary effects. For instance, for the array with 100 RyRs, every RyR has on average 3.6 neighbors, whereas in the small array, with only 16 RyRs, every RyR has on average three neighbors. Thus, the inter-RyR coupling energy acting on every RyR is stronger for RyRs in larger arrays. Second, coupling noise between neighboring RyRs would change the total coupling strength of the RyR array at a certain time point. The second class of modulations mainly affects the single-channel function of the RyR with the results of inactivation or activation of partial RyRs in the array. The activity state of the array is altered in the presence of agonists or antagonists. If the RyRs in the array are strongly coupled with their neighbors, the functional changes of some RyRs may affect the properties of the whole array through activity spread.

It should be noted that the opening and closing of the RyR array is closely related to the coupling state of the neighboring RyRs. The open duration of the RyR array is mainly controlled by the closing reaction of activated RyRs. The functional coupling between activated RyRs will stabilize RyRs at the open state. The factors increasing the coupling strength between activated RyRs would increase the response threshold of the closing reaction of the RyR array, inducing prolonged open duration. On the other hand, factors that decrease the coupling strength between activated RyRs would facilitate the closing of the RyR array, generating a short open duration. Thus, if the coupling state between activated RyRs is easily modulated by perturbations (either increased or decreased), the RyR array cannot show consistent open duration.

In the CC model, the coupling energy could strongly affect the gating of neighboring RyRs and this energy is always there, with no dependence on channel functional states. Thus, coupling energy is an important factor in shaping the dynamics of both opening and closing reactions of the array. Then, the perturbations that alter the total coupling energy of the RyR array, such as array size and coupling noise, would have an obvious influence on RyR array. Also, the functional changes of individual RyRs may be able to affect the properties of the whole array through activity spread through inter-RyR coupling. These two effects function in both the opening and closing processes of the array, and the RyR array with constant coupling thus cannot maintain a consistent open duration against such perturbations.

On the other hand, in the DC model, a decoupling process is induced when RyRs are activated. This means that the inter-RyR coupling is largely decreased with the activation of RyR channels. In this condition, perturbations that change the total coupling strength at the array level would still affect the opening reaction of the array. However, since coupling is not a strong factor that affects the array's opening termination in the DC model, those perturbations would have little effect on the closing reaction of the RyR array. This also applies to the scenario in which the function of some RyRs in the array changes, since functional change of partial

RyRs cannot spread its change to other receptors in the array. Based on these ideas, it is reasonable that consistent open duration of the RyR array can be achieved in the DC model.

Open duration, open probability, and output amplitude of the RyR array are important factors that reflect the signaling performance of arrayed RyRs (21,28). Different from consistent open duration, the RyR arrays with dynamic inter-RyR functional coupling showed tunable open probability and open amplitude in the presence of various perturbations. These results are consistent with the observation that the frequency and amplitude of  $\text{Ca}^{2+}$  sparks are more sensitive to modulators (10–15). As discussed above, open duration of the RyR array largely relies on the closing reaction of the RyRs, whereas open probability and output amplitude are mainly related to the opening reaction of the RyR array. When the gating of RyRs is considered alone, two factors are most important in shaping the opening reaction of the array: single-channel gating and inter-RyR functional coupling. Those modulators that change the activity of individual channels or alter the total coupling state of the RyR array would finally lead to a change in RyR open probabilities. For RyR arrays of different size or RyR arrays with partial channel inactivation, the response amplitude of the array would change accordingly. In the real physiological environment, the open amplitude of RyRs would be affected by many other factors, e.g., SR  $\text{Ca}^{2+}$  content, and thus, actual modulations of the open amplitude should be more complex and tunable.

In this study, we showed that the dynamic inter-RyRs coupling endowed the array system with relatively consistent open duration in the presence of potential perturbations. Furthermore, such an RyR array showed tunable open probability and open amplitude. These results are consistent with in vivo observations of  $\text{Ca}^{2+}$  sparks with consistent RT, and variable frequency and amplitude. The temporally asymmetric modulation of inter-RyR coupling is not only important for the rapid termination of  $\text{Ca}^{2+}$  release, as we proposed in our previous work (21), but also critical for the recapitulation of in vivo characteristic open properties of RyRs. These findings provide further evidence to support dynamic coupling as a feasible in vivo working mechanism of RyR arrays. Moreover, dynamic coupling is also believed to be a potential strategy for endowing a biological system with properties that are robust to external noises, which generally makes certain sense in understanding the control theory of biological systems in physiology.

This work was supported by a grant from the National Nature Science Foundation of China (NSFC30670495), the Ministry of Science and Technology of China (2006CB0D0100), and a 985 Project from Shanghai Jiao Tong University.

## REFERENCES

1. Rios, E., and G. Pizarro. 1991. Voltage sensor of excitation-contraction coupling in skeletal muscle. *Physiol. Rev.* 71:849–908.

2. Meissner, G. 1994. Ryanodine receptor/ $\text{Ca}^{2+}$  release channels and their regulation by endogenous effectors. *Annu. Rev. Physiol.* 56:485–508.
3. Bers, D. M. 2002. Cardiac excitation-contraction coupling. *Nature*. 415:198–205.
4. Fill, M., and J. A. Copello. 2002. Ryanodine receptor calcium release channels. *Physiol. Rev.* 82:893–922.
5. Franzini-Armstrong, C., F. Protasi, and V. Ramesh. 1999. Shape, size, and distribution of  $\text{Ca}^{2+}$  release units and couplons in skeletal and cardiac muscles. *Biophys. J.* 77:1528–1539.
6. Yin, C. C., and F. A. Lai. 2000. Intrinsic lattice formation by the ryanodine receptor calcium-release channel. *Nat. Cell Biol.* 2:669–671.
7. Takekura, H., and C. Franzini-Armstrong. 2002. The structure of  $\text{Ca}^{2+}$  release units in arthropod body muscle indicates an indirect mechanism for excitation-contraction coupling. *Biophys. J.* 83:2742–2753.
8. Wang, S. Q., L. S. Song, L. Xu, G. Meissner, E. G. Lakatta, et al. 2002. Thermodynamically irreversible gating of ryanodine receptors in situ revealed by stereotyped duration of release in  $\text{Ca}^{2+}$  sparks. *Biophys. J.* 83:242–251.
9. Wang, S. Q., M. D. Stern, E. Rios, and H. Cheng. 2004. The quantal nature of  $\text{Ca}^{2+}$  sparks and in situ operation of the ryanodine receptor array in cardiac cells. *Proc. Natl. Acad. Sci. USA*. 101:3979–3984.
10. Shen, J. X., S. Wang, L. S. Song, T. Han, and H. Cheng. 2004. Polymorphism of  $\text{Ca}^{2+}$  sparks evoked from in-focus  $\text{Ca}^{2+}$  release units in cardiac myocytes. *Biophys. J.* 86:182–190.
11. Lacampagne, A., M. G. Klein, C. W. Ward, and M. F. Schneider. 2000. Two mechanisms for termination of individual  $\text{Ca}^{2+}$  sparks in skeletal muscle. *Proc. Natl. Acad. Sci. USA*. 97:7823–7828.
12. Yang, Z., and D. S. Steele. 2001. Effects of cytosolic ATP on  $\text{Ca}^{2+}$  sparks and SR  $\text{Ca}^{2+}$  content in permeabilized cardiac myocytes. *Circ. Res.* 89:526–533.
13. Zhou, J., B. S. Launikonis, E. Rios, and G. Brum. 2004. Regulation of  $\text{Ca}^{2+}$  sparks by  $\text{Ca}^{2+}$  and  $\text{Mg}^{2+}$  in mammalian and amphibian muscle. An RyR isoform-specific role in excitation-contraction coupling? *J. Gen. Physiol.* 124:409–428.
14. Zhang, Y., G. G. Rodney, and M. F. Schneider. 2005. Effects of azumolene on  $\text{Ca}^{2+}$  sparks in skeletal muscle fibers. *J. Pharmacol. Exp. Ther.* 314:94–102.
15. Rodney, G. G., and M. F. Schneider. 2003. Calmodulin modulates initiation but not termination of spontaneous  $\text{Ca}^{2+}$  sparks in frog skeletal muscle. *Biophys. J.* 85:921–932.
16. Marx, S. O., J. Gaburjakova, M. Gaburjakova, C. Henrikson, K. Ondrias, et al. 2001. Coupled gating between cardiac calcium release channels (ryanodine receptors). *Circ. Res.* 88:1151–1158.
17. Xu, L., and G. Meissner. 1998. Regulation of cardiac muscle  $\text{Ca}^{2+}$  release channel by sarcoplasmic reticulum luminal  $\text{Ca}^{2+}$ . *Biophys. J.* 75:2302–2312.
18. Yin, C. C., L. G. D'Cruz, and F. A. Lai. 2008. Ryanodine receptor arrays: not just a pretty pattern? *Trends Cell Biol.* 18:149–156.
19. Marx, S. O., K. Ondrias, and A. R. Marks. 1998. Coupled gating between individual skeletal muscle  $\text{Ca}^{2+}$  release channels (ryanodine receptors). *Science*. 281:818–821.
20. Hu, X. F., X. Liang, K. Y. Chen, H. Xie, Y. Xu, et al. 2005. Modulation of the oligomerization of isolated ryanodine receptors by their functional states. *Biophys. J.* 89:1692–1699.
21. Liang, X., X. F. Hu, and J. Hu. 2007. Dynamic interreceptor coupling: a novel working mechanism of two-dimensional ryanodine receptor array. *Biophys. J.* 92:1215–1223.
22. Bers, D. M., and V. M. Stiffel. 1993. Ratio of ryanodine to dihydropyridine receptors in cardiac and skeletal muscle and implications for E-C coupling. *Am. J. Physiol.* 264:C1587–C1593.
23. Xie, H., and P. H. Zhu. 2006. Biphasic modulation of ryanodine receptors by sulfhydryl oxidation in rat ventricular myocytes. *Biophys. J.* 91:2882–2891.
24. Blatter, L. A., J. Huser, and E. Rios. 1997. Sarcoplasmic reticulum  $\text{Ca}^{2+}$  release flux underlying  $\text{Ca}^{2+}$  sparks in cardiac muscle. *Proc. Natl. Acad. Sci. USA*. 94:4176–4181.
25. Rios, E., M. D. Stern, A. Gonzalez, G. Pizarro, and N. Shirokova. 1999. Calcium release flux underlying  $\text{Ca}^{2+}$  sparks of frog skeletal muscle. *J. Gen. Physiol.* 114:31–48.
26. Rios, E., and G. Brum. 2002.  $\text{Ca}^{2+}$  release flux underlying  $\text{Ca}^{2+}$  transients and  $\text{Ca}^{2+}$  sparks in skeletal muscle. *Front. Biosci.* 7:d1195–d1211.
27. Fu, Y., G. Q. Zhang, X. M. Hao, C. H. Wu, Z. Chai, et al. 2005. Temperature dependence and thermodynamic properties of  $\text{Ca}^{2+}$  sparks in rat cardiomyocytes. *Biophys. J.* 89:2533–2541.
28. Smith, G. D., J. E. Keizer, M. D. Stern, W. J. Lederer, and H. Cheng. 1998. A simple numerical model of calcium spark formation and detection in cardiac myocytes. *Biophys. J.* 75:15–32.